Altered expression of the *IGF2-H19* locus and mitochondrial respiratory complexes in adrenocortical carcinoma

PATRICK SCICLUNA[1,2], STEFANO CARAMUTA[1], HANNA KJELLIN[3,4], CHENG XU[3], ROBIN FRÖBOM[3], MONIRA AKHTAR[5], JIWEI GAO[1], HAO SHI[1], MAGNUS KJELLMAN[3,6], MALIN ALMGREN[5], ANDERS HÖÖG[1,7], JAN ZEDENIUS[3,6], TOMAS J. EKSTRÖM[3], ROBERT BRÄNSTRÖM[3,6], WENG-ONN LUI[1] and CATHARINA LARSSON[1,7]

[1]Department of Oncology-Pathology, BioClinicum, Karolinska University Hospital, Karolinska Institutet, SE-171 64 Solna; [2]Department of Cell and Molecular Biology, Karolinska Institutet, SE-171 65 Stockholm; [3]Department of Molecular Medicine and Surgery, Karolinska Institutet, SE-171 76 Stockholm; [4]Science for Life Laboratory, Cancer Proteomics Mass Spectrometry, Karolinska Institutet, SE-171 21 Solna; [5]Department of Clinical Neuroscience, Karolinska Institutet; [6]Department of Breast, Endocrine Tumors and Sarcoma, Karolinska University Hospital; [7]Department of Clinical Pathology and Cancer Diagnostics, Karolinska University Hospital, SE-171 76 Stockholm, Sweden

Received June 30, 2022; Accepted August 31, 2022

DOI: 10.3892/ijo.2022.5430

Abstract. Abnormalities of the insulin-like growth factor 2 (*IGF2*)-*H19* locus with the overexpression of *IGF2* are frequent findings in adrenocortical carcinoma (ACC). The present study assessed the expression of RNAs and microRNAs (miRNAs/miRs) from the *IGF2-H19* locus using PCR-based methods in ACC and adrenocortical adenoma (ACA). The results were associated with proteomics data. *IGF2* was overexpressed in ACC, and its expression correlated with that of *miR-483-3p* and *miR-483-5p* hosted by *IGF2*. The downregulated expression of *H19* in ACC compared to ACA correlated with *miR-675* expression hosted by *H19*. Several proteins exhibited an inverse correlation in expression and were predicted as targets of *miR-483-3p*, *miR-483-5p* or *miR-675*. Subsets of these proteins were differentially expressed between ACC and ACA. These included several proteins involved in mitochondrial metabolism. Among the mitochondrial respiratory complexes, complex I and IV were significantly decreased in ACC compared to ACA. The protein expression of NADH:ubiquinone oxidoreductase subunit C1 (NDUFC1), a subunit of mitochondrial respiratory complex I, was further validated as being lower in ACC compared to ACA and normal adrenals. The silencing of *miR-483-5p* increased NDUFC1 protein expression and reduced both oxygen consumption and glycolysis rates. On the whole, the findings of the present study reveal the dysregulation of the *IGF2-H19* locus and mitochondrial respiration in ACC. These findings may provide a basis for the further understanding of the pathogenesis of ACC and may have potential values for diagnostics and treatment.

Correspondence to: Dr Weng-Onn Lui or Dr Catharina Larsson, Department of Oncology-Pathology, BioClinicum J6:20, Karolinska University Hospital, Karolinska Institutet, SE-171 64 Solna, Sweden
E-mail: weng-onn.lui@ki.se
E-mail: catharina.larsson@ki.se

Key words: adrenal cortical tumors, insulin-like growth factor 2, H19, microRNAs, mitochondrial respiratory complexes

Introduction

Adrenocortical carcinoma (ACC) is a rare, yet highly aggressive tumor type (1). In addition to gross genomic alterations, mutational events in several key genes involved in the β-catenin pathway (e.g., *CTNNB1* and *ZNRF3*), the p53/Rb pathway (e.g., *TP53*, *CDKN2A* and *RB1*) and chromatin remodeling (e.g., *MEN1, TERT* and *DAXX*) are associated with ACC tumorigenesis (1-3). The overexpression of insulin-like growth factor (IGF) II and the *IGF2* gene is observed in the majority of ACC; however, this does not occur in adrenocortical adenoma (ACA) or normal adrenal glands (4-6).

The *IGF2* gene is located within 90 kb from the *H19* gene in chromosomal region 11p15.5 (7). *H19* produces an untranslated, yet spliced and polyadenylated transcript with possible tumor suppressor function (8), and *IGF2* encodes the growth factor, IGFII. The *IGF2-H19* locus is subjected to parental imprinting, which is frequently lost in cancer by the loss of imprinting, leading to the overexpression of *IGF2*/IGFII (9-11). Furthermore, IGFII has been reported to promote malignant transformation in the mammary gland *in vivo* (12). However, it has not been found to exert an effect on the tumor phenotype *in vitro* (13), and only mildly contributes to the development of ACC *in vivo* (14,15). Given that IGFII acts on the IGF1 receptor (IGF1R), the application of an IGF1R blocker has been attempted in anticancer therapy to counteract IGFII signaling in ACC (16-21). In ACC, *H19* expression has been reported to be decreased as compared to that in ACA (6), while *IGF2*/IGFII expression is known to be markedly increased in the vast majority of ACC cases (4,6,22-24).

MicroRNAs (miRNAs/miRs) are short non-coding RNAs that generally suppress the expression of target genes by mRNA degradation or translational repression (25). Three miRNAs are known to be transcribed from the *IGF2-H19* locus, i.e., *miR-483-3p* and *miR-483-5p* from *IGF2* intron 7, and *miR-675* from *H19*. *miR-483-3p* is overexpressed in different tumor types, including ACC (13,26-28). Furthermore, the p53 upregulated modulator of apoptosis (PUMA) is a target of *miR-483-3p,* and the inhibition of *miR-483-3p* inhibits proliferation and increases apoptosis *in vitro*, and tumorigenicity *in vivo* (13,27). *miR-483-5p* is also overexpressed in ACC (26-29) and their inhibition *in vitro* reduces cell growth, although it does not affect the apoptosis of ACC cells (27). On the other hand, *miR-483-5p* has been shown to regulate the N-Myc downstream-regulated gene 2 and promote the invasion of ACC cells (30). Notably, *miR-483-5p* is detectable in serum samples of patients with ACC, and its high expression level is associated with a degree of malignancy and a poor survival (31-33). The overexpression of *miR-675* has been reported in various types of cancer, e.g. gastric, colorectal, esophageal and breast cancer (34-37); however, the decreased expression has also been observed in non-small cell lung cancer (38). In adrenocortical tumors, *miR-675* has only been analyzed in a small cohort of 13 patients (4 patients with ACC and 9 patients with ACA), while the significance of its deregulation in ACC remains to be investigated (39).

The present study aimed to comprehensively characterize the expression of RNAs and miRNAs generated from the *IGF2-H19* locus in adrenocortical tissues and associate their expression levels with global protein expression profiles in ACA and ACC. The analysis revealed the expression of several proteins involved in mitochondrial respiratory complexes that inversely correlated with the *miR-483-5p* level. Functionally, *miR-483-5p* was demonstrated to regulate the expression of the NADH:ubiquinone oxidoreductase subunit C1 (NDUFC1) and the mitochondrial oxygen consumption rate.

Materials and methods

Tissue material. Fresh-frozen tumor tissues were obtained from the Karolinska University Hospital Biobank for patients treated surgically for ACC (n=35) or ACA (n=43) between 1986 and 2010. Tumors were classified according to the WHO criteria (40). In addition, normal adrenal gland samples were obtained from patients undergoing nephrectomy for other reasons, or from patients with adrenocortical tumors, and histologically verified as non-malignant. The samples were obtained with informed consent and the study of the tissue material was approved by the Ethical Committee of the Karolinska University Hospital.

The clinical information for all cases is presented in Table SI. The screening series included 6 cases with ACA and 8 cases with ACC used for proteomics analysis in a previous study by the authors (41). An extended series of samples from nine normal adrenal glands, 43 ACA and 29 ACC (30 samples) was used for the reverse transcription-quantitative PCR (RT-qPCR) analysis of RNAs and miRNAs. The results from the quantification analyses of *miR-483-3p* and *miR-483-5p* have been previously published for most cases (27). Additionally, samples from 13 normal adrenal glands, 25 ACA and 25 ACC (29 samples) were used for western blot analyses. The ACA and ACC cases included in the different analyses are presented in Table SI.

Data analysis from TCGA and genotype-tissue expression (GTEx). Comparisons of *IGF2* or *H19* RNA expression levels between ACCs and normal adrenal glands, and principal component analysis (PCA) were performed in Gene Expression Profiling Interactive Analysis [GEPIA; (42)]. The RNA expression levels were based on the RNA sequencing expression data of 77 ACC cases from The Cancer Genome Atlas (TCGA) and 128 normal adrenal glands from GTEx. PCA was performed using the 46 genes whose proteins inversely correlated with *miR-483-5p* and significantly differentially expressed between ACA and ACC ($P<0.05$, Table SII). Correlations between the expression of *IGF2* and *H19*, *IGF2* and *miR-483-3p* or *miR-483-5p*, *H19* and *miR-675* were assessed in the StarBase Pan-Cancer Analysis Platform (43). This platform includes RNA and miRNA sequencing data of 79 ACC samples from TCGA.

Cell line and cell culture. All *in vitro* cell assays were performed using the NCI-H295R ACC cell line purchased from the American Type Culture Collection (cat. no. CRL-2128; ATCC). The cells were maintained in DMEM:F12 medium (cat. no. 31330038; Gibco; Thermo Fisher Scientific, Inc.) supplemented with 2.5% NuSerum Growth medium (Corning 355100; Thermo Fisher Scientific, Inc.) and 1% insulin-transferrin-selenium basal medium supplement (cat. no. 41400045; Thermo Fisher Scientific, Inc.). The cells were incubated at 37˚C in a humidified CO_2 incubator. The authenticity of the cell line was re-verified prior to the experiments by genotyping of short tandem repeats (STRs) performed by the National Genomics Infrastructure-Uppsala (SciLifeLab, Uppsala University, Uppsala, Sweden). The NCI-H295R cell line is the only human ACC cell line that is capable of secreting major adrenocortical steroids (44), representing the cellular origin of ACC cells, and it is the most extensively used cell line in *in vitro* models of ACC.

RT-qPCR analysis. The expression levels of mature miRNAs and RNAs were evaluated using RT-qPCR with an Applied Biosystems 7900HT Fast Real-Time PCR System (Applied Biosystems; Thermo Fisher Scientific, Inc.). cDNA for miRNA analysis was synthesized from 25 ng total RNA using the TaqMan MicroRNA Reverse Transcription kit (Applied Biosystems; Thermo Fisher Scientific, Inc.). miRNA assays for *miR-483-3p* (ID 002339), *miR-483-5p* (ID 002338) and *miR-675* (ID 002005) were purchased from Applied Biosystems (Thermo Fisher Scientific, Inc.) and normalization was performed using *RNU6B* (ID 001093). The high Capacity cDNA Reverse Transcription kit (Applied Biosystems; Thermo Fisher Scientific, Inc.) was adopted to generate cDNA from 100 ng total RNA for RNA expression analysis and specific TaqMan probes targeting *IGF2* (ID 00277496_s1) and *H19* (ID 00399293_g1) were used for RT-qPCR. Normalization was performed using *18S* (ID 99999901). All TaqMan probes were labeled with FAM-MGB (Applied Biosystems); the reverse transcription and qPCR conditions followed the manufacturer's instructions. All reactions were performed in triplicate and the relative expression levels were determined using the $\Delta\Delta C_q$ method and reported as $2^{-\Delta\Delta Cq}$ (45).

Proteomics data analysis. Proteomics profiling for 6 cases of ACA and 8 cases of ACC in the screening series has been described in a previous study by the authors (41). The protein expression levels of the screening series were correlated with their corresponding *IGF2*, *H19*, *miR-483-3p*, *miR-483-5p* and *miR-675* transcripts using Pearson's correlation analysis. The mRNA targets of *miR-483-3p*, *miR-483-5p* and *miR-675* were predicted using TargetScan 7.1 (https://www.targetscan.org/vert_71/). Ingenuity pathway analysis of complex 'omics' data (IPA; IPA version 14400082; Ingenuity® Systems, www.ingenuity.com) was employed to assess the theoretical interactions and cellular networks of the proteins that correlated with *IGF2*.

Gene ontology (GO) enrichment analysis. The gene signature corresponding to the 46 proteins that inversely correlated with *miR-483-5p*, and significantly differentially expressed between ACA and ACC in the proteomics cohort (Table SII) was annotated based on biological processes using GO enrichment analysis (http://geneontology.org/). The analysis was based on the PANTHER overrepresentation test (released on August 3, 2019; http://www.pantherdb.org/) and the GO database (released on February 2, 2019). P-values <0.05 following the Bonferroni correction were considered to indicate statistically significant differences.

Transfections with miRNA inhibitors. Transfections were performed by suspending $3x10^6$ NCI-H295R cells in 100 μl Ingenio solution (Mirus Bio) together with 100 pmol mirVana *miR-483-5p* inhibitor, *miR-483-3p* inhibitor or Negative Control #1 (MH12629, MH12478 and 4464076, respectively; Thermo Fisher Scientific, Inc.) in Ingenio cuvettes (MIR50121; Mirus Bio). The cells were electroporated using the program T-20 of the Amaxa Nucleofector device (Lonza Group, Ltd.) and then transferred into a culture plate containing pre-warmed complete DMEM:F12 medium. The plate was incubated at 37˚C in a humidified CO_2 incubator. The cell culture medium was replaced at 24 h post-transfection and harvested for metabolic profiling or western blot analysis following 48 h of transfection. At least three biological replicates were performed for each transfection. The efficiency of *miR-483-5p* silencing was assessed using RT-qPCR.

Real-time metabolic profiling. Mitochondrial and glycolytic functions were measured using the Mito Stress Test and Glycolysis Stress Test, respectively (Agilent Technologies, Inc.) using the Seahorse XFe24 Analyser (Agilent Technologies, Inc.). The transfected cells were seeded at $1.5x10^5$/well in 24-well plates (Seahorse XF24 V7 PS Culture Microplates, Agilent Technologies, Inc.). The culture media were replaced after 24 h and incubated for a further 24 h at 37˚C. Culture media were changed to the Seahorse XF Base Medium (Agilent Technologies, Inc.) supplemented with 5.5 mM glucose, 1 mM L-glutamine and 1 mM sodium pyruvate at pH 7.4 and incubated at 37˚C with CO_2 for 1 h. For the evaluation of mitochondrial respiration, the oxygen consumption rate (OCR) was measured at the basal level and following sequential loading with 1 μM oligomycin (ATP synthase inhibitor), 0.5 μM carbonyl cyanide p-trifluoromethoxy-phenylhydrazone (FCCP, an uncoupler of oxidative phosphorylation), 1 μM rotenone and antimycin A (complex I and III inhibitor, respectively). For the assessment of glycolysis, the extracellular acidification rate (ECAR) was analyzed at basal conditions and after sequential loading with 1 μM oligomycin (inhibiting ATP synthase in the mitochondria leading to enhanced glycolysis dependency), and 50 mM 2-deoxyglucose (2-DG, a competitive inhibitor of glucose). Both OCR and ECAR were normalized to the total protein content in each well as measured using the Bradford assay (Bio-Rad Laboratories, Inc.).

Western blot analysis. Cell pellets or tissue samples were suspended in RIPA lysis and extraction buffer (cat. no. 89901; Thermo Fisher Scientific, Inc.) supplemented with 1 mM phenylmethanesulfonyl fluoride (PMSF; Sigma-Aldrich; Merck KGaA), 1% cOmplete™ proteinase inhibitor cocktail (Sigma-Aldrich; Merck KGaA) and 1% phosphatase inhibitor cocktail 2 and 3 (Sigma-Aldrich; Merck KGaA). The lysates were vortexed repeatedly and left on ice for 60 min or until homogenization. The protein concentration was quantified using the Bradford assay (Bio-Rad Laboratories). Denatured lysates (40 μg) were separated in 10% NuPAGE™ Bis-Tris denaturing pre-cast gels (Invitrogen; Thermo Fisher Scientific, Inc.) and transferred onto nitrocellulose membranes (cat. no. 88013, Thermo Fisher Scientific, Inc.) at 4˚C. The membranes were blocked in 5% BSA or 1% non-fat dried milk (for total OXPHOS WB) in TBS containing 0.1% Tween-20 (Sigma-Aldrich; Merck KGaA). The membranes were then incubated overnight at 4˚C with the primary antibodies, anti-NDUFC1 (cat. no. PA5-68240; Thermo Fisher Scientific, Inc.) at a 1:500 dilution and total OXPHOS WB Antibody Cocktail (ab110413, Abcam) at a 1:250 dilution. Anti-β-actin (A1978, Sigma-Aldrich; Merck KGaA) diluted to 1:2,500 was used for normalization purposes. IRDye 800CW goat anti-mouse IgG (LI-COR Biosciences) at a 1:10,000 dilution or HRP-conjugated goat anti-rabbit IgG (cat. no. 31466, Invitrogen; Thermo Fisher Scientific, Inc.) at a 1:2,000 dilution or goat anti-mouse IgG (cat. no. 62-6520 Invitrogen; Thermo Fisher Scientific, Inc.) at a 1:10,000 dilution were used as secondary antibodies. Novex Sharp pre-stained protein standard (LC5800, Thermo Fisher Scientific, Inc.) and Precision Plus Protein All Blue protein standards were used as molecular weight markers. Chemiluminescent signals were detected using the SuperSignal™ West Femto Maximum Sensitivity Substrate (cat. no. 34096, Thermo Fisher Scientific, Inc.) and the Odyssey Fc imaging system (LI-COR Biosciences) and quantified using Image Studio Lite 5.2 software (LI-COR Biosciences).

Statistical analyses. Statistica 10.0 (StatSoft, Inc., Tulsa, OK) or IBM SPSS Statistics version 24.0 (IBM Corp., Armonk, NY) was used for all statistical analyses, unless otherwise specified. Differences in expression levels between two sample groups were calculated using the Mann-Whitney U-test or the Student's t-test. One-way ANOVA with post hoc Tukey's test was used to compare the three transfection conditions for the metabolic assays. Correlations between *IGF2* and *H19* and miRNA (*miR-483-3p*, *miR-483-5p* and *miR-675*) expression levels were assessed using Spearman's rank order correlation analysis. Difference in NDUFC1 levels in transfection experiments were evaluated using the Student's t-test. All

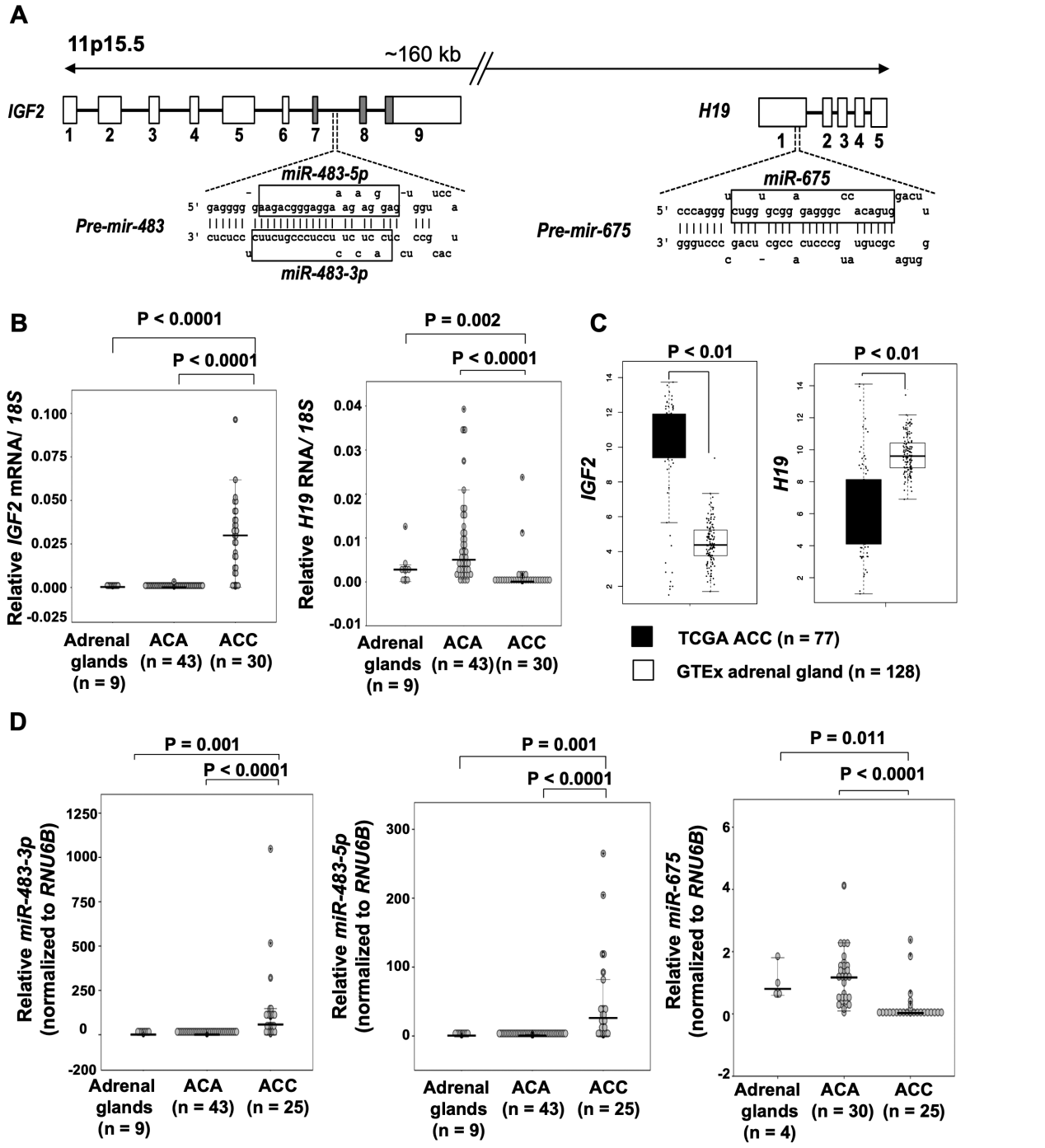

Figure 1. Expression from the *IGF2-H19* locus in adrenocortical tumors and normal adrenals. (A) Schematic illustration of the *IGF2-H19* locus in human chromosomal region 11p15.5. The *IGF2* gene generates the IGFII protein translated from the common coding exons 7, 8 and 9 (grey). *miR-483-3p* and *miR-483-5p* are transcribed from *IGF2* intron 7 and *H19* generates *miR-675*. (B and C) Graphic representation of relative expression levels of *IGF2* and *H19* RNAs determined using reverse transcription-quantitative PCR in ACC, ACA and normal adrenal tissue samples of (B) the present study cohort and (C) employing the data from TCGA and GTEx. (D) Relative miRNA expression levels of *miR-483-3p*, *miR-483-5p* and *miR-675* in the present cohort. P-values <0.05 were considered to indicate statistically significant differences, as determined using the Mann-Whitney U-test. *IGF2*, insulin-like growth factor 2; ACC, adrenocortical carcinoma; ACA, adrenocortical adenoma; TCGA, from The Cancer Genome Atlas; GTEx, Genotype-Tissue Expression.

analyses were two-tailed and P-values <0.05 were considered to indicate statistically significant differences.

Results

Expression of RNAs and miRNAs from the IGF2-H19 locus. The RNA and miRNA transcripts generated from *IGF2* and *H19* (Fig. 1A) were quantified using RT-qPCR in an extended series of normal adrenal glands, ACAs and ACCs. The results are illustrated in Fig. 1B-D. Elevated levels of *IGF2* and decreased levels of *H19* were observed in the majority of ACC tissues as compared to ACA tissues and normal adrenals. Concordant with the findings in the present cohort, the ACC samples (n=77) in TCGA dataset also exhibited higher levels

of *IGF2* RNA and lower levels of *H19*, as compared to normal adrenal glands from the GTEx (n=128) datasets. *miR-483-3p* and *miR-483-5p* generated from *IGF2* were both upregulated in ACC vs. ACA and normal adrenals, as previously published for a subset of the cases (27). *miR-675* transcribed from *H19* was underexpressed in ACC as compared to ACA and normal adrenals.

A comparison of the RNAs and miRNAs analyzed in the extended series of normal adrenal glands, ACA and ACC revealed a moderately inverse correlation between *IGF2* and *H19* (Fig. 2A). Strong positive correlations were found between *miR-483-3p* and *miR-483-5p* and their host *IGF2*, as well as between *miR-675* and its host *H19* (Fig. 2A). Similar findings were subsequently revealed in TCGA dataset with 79 ACC cases (Fig. 2B). A weak inverse correlation, although not statistically significant, was observed between *H19* and *IGF2*. Strong positive correlations were observed between *IGF2* and *miR-483-3p* and *miR-483-5p*, as well as between *H19* and *miR-675*.

Comparative analysis of transcripts with the proteome. Protein expression profiles determined using mass spectrometry for the 6 cases of ACA and 8 cases of ACC in the screening series (41) were compared with the expression levels of the RNAs (*IGF2* and *H19*) and miRNAs (*miR-483-3p*, *miR-483-5p* and *miR-675*). The numbers of proteins overlapping with the various transcripts are illustrated in Venn diagrams in Fig. 3A and B. In total, six proteins were associated with both *IGF2* and *miR-483-3p*, 48 proteins were associated with *IGF2* and *miR-483-5p*, and 120 proteins were associated with *IGF2* and both *miR-483-3p* and *miR-483-5p*. Only four proteins were associated with *H19* and *miR-675*.

A comparison of the proteomics data with the expression of *IGF2* or *H19* identified 222 proteins that correlated with *IGF2* (Table SIII) and 71 that correlated with *H19* (Table SIV). The proteomics data were also investigated to identify proteins exhibiting an inverse expression to the three miRNAs, since such proteins would represent potential targets. This identified seven proteins whose expression inversely correlated with that of *miR-483-3p*, including one predicted target using TargetScan 7.1 (Table SV). For *miR-483-5p*, 101 inversely correlated proteins were revealed including nine predicted targets (Table SII). For *miR-675*, 11 inversely expressed proteins were identified, including one predicted target (Table SVI).

Among the 101 proteins that were inversely correlated with *miR-483-5p*, 46 of them were differentially expressed between ACA and ACC based on the proteomics data (Table SII). Based on these 46 protein expression patterns, all ACC cases (apart from ACC case no. 10) were clustered together and separated from the ACA cluster (Fig. 3C). Using TCGA and GTEx datasets, it was also observed that this 46-gene signature could distinguish ACC from normal adrenal glands (Fig. 3D). GO analysis of these 46 genes revealed a significant enrichment of biological processes related to mitochondrial metabolism (Fig. 3E). Notably, six proteins (NDUFV1, NDUFC1, NDUFC2, NDUFB9, NDUFB3 and NDUFB7) are subunits of the mitochondrial respiratory chain complex I. Among these six subunits, only NDUFC1 is a predicted target of *miR-483-5p* according to TargetScan 7.1.

Protein expression of mitochondrial respiratory complexes in adrenal cortical tissues. To further assess the association between mitochondrial respiratory complexes and ACC, the expression levels of mitochondrial respiratory complex I-V were examined in nine adrenal glands, 10 ACA tissues and 10 ACC tissues using western blot analysis, and the total OXPHOS antibody cocktail representing each of the complexes (Fig. 4A). Of note, complex I and IV were lower in ACC compared to ACA (P=0.009 and P=0.002, respectively; Fig. 4B). On the other hand, complex II and III were higher in ACC compared to adrenal glands (P=0.013 and P=0.008, respectively), whereas they did not differ significantly compared to ACA (Fig. 4B).

To validate the involvement of complex I in ACCs, NDUFC1 protein expression was also evaluated in an extended series of clinical samples, consisting of 13 normal adrenal glands, 25 ACA and 29 ACC samples (from 25 patients with ACC), using western blot analysis (Fig. 4C). Concordantly, NDUFC1 expression was lower in ACC compared to ACA and normal adrenals (P=0.043 and P=0.046, respectively; Fig. 4D). The inhibition of *miR-483-5p,* using anti-miR-483-5p, in the NCI-H295R ACC cell line increased NDUFC1 protein expression (Fig. 4E and F), suggesting a putative role of *miR-483-5p* in mitochondrial respiratory activities.

Role of miR-483 in the cellular metabolism of ACC cells. To further validate the effects of *miR-483-5p* on metabolic activities, the mitochondrial OCR and ECAR were measured using a Seahorse system. The OCR profile exhibited a significant decrease in the basal and maximum respiration upon the inhibition of *miR-483-5p*, but not that of *miR-483-3p*, using anti-miR-483-5p and anti-miR-483-3p, respectively (Fig. 5A and B). Additionally, ATP production generated from the mitochondrial respiration was also lower in the cells transfected with anti-miR-483-5p, compared to those transfected with anti-miR-483-3p or negative control-transfected cells (Fig. 5B).

The measurement of the ECAR, an indicator of glycolysis, revealed a decrease in basal glycolysis, glycolytic capacity and reserve in the anti-miR-483-5p-transfected cells. Similar effects were also observed upon the inhibition of *miR-483-3p* (Fig. 5A and B). To obtain an overview of the bioenergetics profile, the OCR vs. ECAR was plotted at basal conditions. As illustrated in Fig. 5C, the cells in which *miR-483-5p* was inhibited were least energetic, as demonstrated by lower respiration and glycolysis rates, whereas the cells in which *miR-483-3p* was inhibited were less glycolytic, but were similarly oxidative as the anti-miR-CTR-transfected cells.

Discussion

Several studies have demonstrated that the overexpression of *IGF2* is a very frequent alteration in ACC, which suggests a role for this growth factor in ACC tumor development (4-6). The present study further analyzed this alteration by measuring RNA and miRNA transcripts from the *IGF2* and *H19* loci and associated these results with global protein levels determined using proteomics. The present study confirmed previous findings (4,5) that *IGF2* expression is elevated in ACC compared to normal adrenal and to ACA. The higher transcription of *IGF2* was, as expected, paralleled by an increased expression of *miR-483-3p* and *miR-483-5p* (hosted by *IGF2*) in ACC.

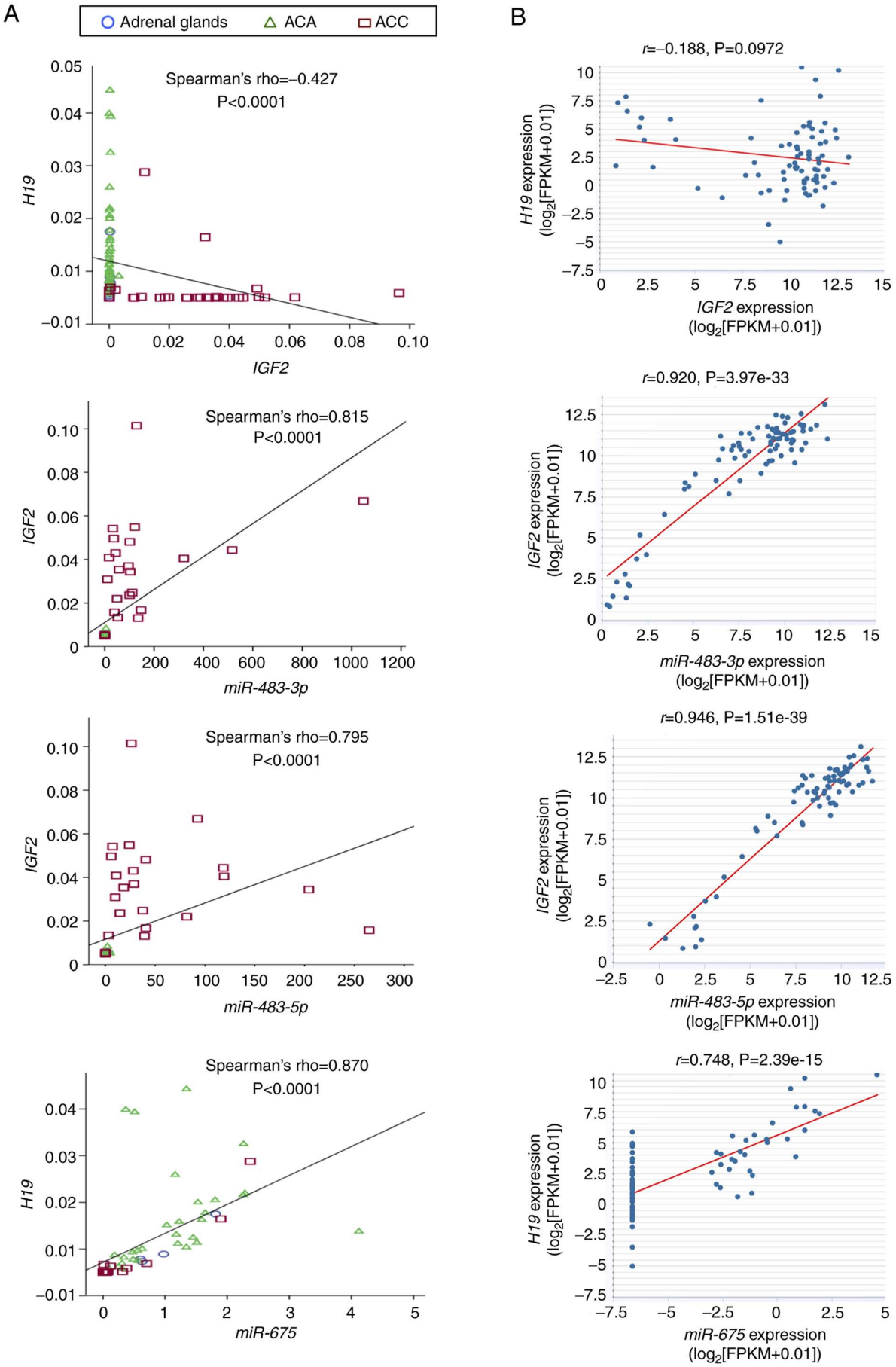

Figure 2. Correlation analysis between the RNA expression levels of the host genes *IGF2* and *H19*, and their hosted miRNAs *miR-483-3p*, *miR-483-5p* and *miR-675*. (A) Results from the complete series of normal adrenal, ACA and ACC. (B) Correlation analyses of data for 79 ACC obtained from The Cancer Genome Atlas. *IGF2*, insulin-like growth factor 2; ACC, adrenocortical carcinoma; ACA, adrenocortical adenoma.

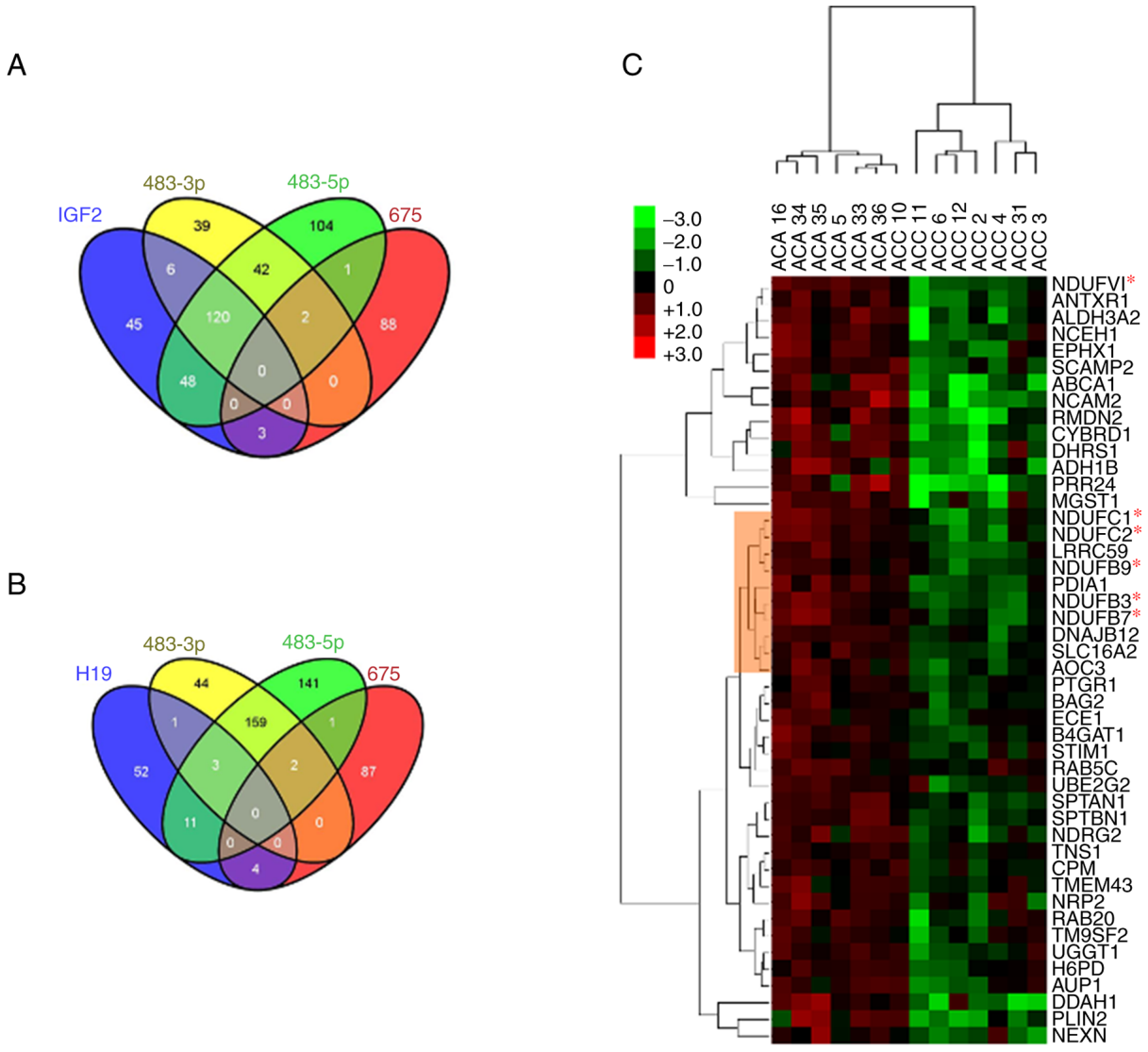

E

GO biological process	Count	Fold enrichment	*P*-value*
Mitochondrial electron transport, NADH to ubiquinone (GO:0006120)	6	63.62	8.74E-06
Oxidation-reduction process (GO:0055114)	14	6.9	5.97E-05
NADH dehydrogenase complex assembly (GO:0010257)	6	42.42	8.30E-05
Mitochondrial respiratory chain complex I assembly (GO:0032981)	6	42.42	8.30E-05
Mitochondrial ATP synthesis coupled electron transport (GO:0042775)	6	34.56	2.62E-04
ATP synthesis coupled electron transport (GO:0042773)	6	34.14	2.81E-04
Mitochondrial respiratory chain complex assembly (GO:0033108)	6	28.28	8.11E-04
Respiratory electron transport chain (GO:0022904)	6	27.99	8.58E-04
Oxidative phosphorylation (GO:0006119)	6	26.92	1.07E-03
Cellular respiration (GO:0045333)	6	17.83	1.09E-02
Electron transport chain (GO:0022900)	6	15.47	2.42E-02
Small molecule metabolic process (GO:0044281)	15	3.85	2.85E-02
ATP metabolic process (GO:0046034)	6	14.66	3.27E-02

*Bonferroni-corrected *P*-value

Figure 3. Comparative analysis of transcripts with the proteome in the screening cohort. (A and B) Venn diagrams illustrating the number of proteins overlapping between (A) *IGF2* and (B) *H19* with *miR-483-3p*, *miR-483-5p* and *miR-675*, as determined using proteomics analysis as previously described (41). (C) Clustering analysis of the 14 adrenocortical tumors (6 cases of ACA and 8 cases of ACC) using the 46 proteins that were inversely correlated with *miR-483-5p* and differentially expressed between ACC and ACA. Samples were clustered using the Spearman's rank order correlation with complete linkage. Red and green indicate relatively high and low expression, respectively. The cluster highlighted in orange consists of proteins related to mitochondrial metabolism. Proteins associated with mitochondrial respiratory complex I are marked with an asterisk (*). (D) Principal component analysis of the 77 cases of ACC from The Cancer Genome Atlas and 128 adrenal glands from Genotype-Tissue Expression using the 46-gene signature corresponding to the proteins inversely correlating with *miR-483-5p* and differentially expressed between ACC and ACA. (E) The 46-gene signature was functionally annotated and analyzed using the PANTHER overrepresentation test with Bonferroni correction. *IGF2*, insulin-like growth factor 2; ACC, adrenocortical carcinoma; ACA, adrenocortical adenoma.

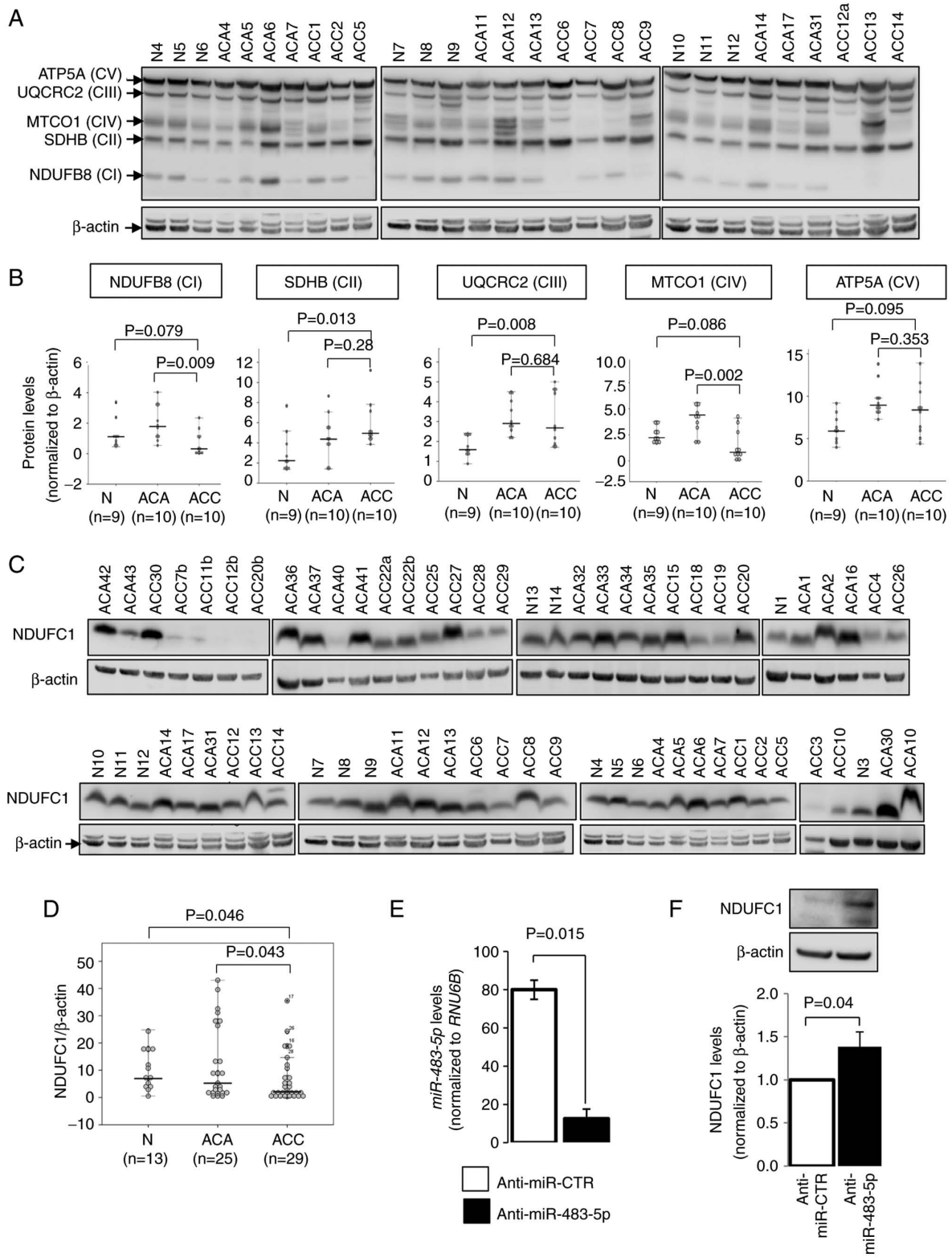

Figure 4. Expression levels of mitochondrial respiratory complexes in normal adrenals and adrenocortical tumors, and the effect of *miR-483-5p* on NDUFC1. (A) Mitochondrial respiratory complexes I-V were evaluated in nine adrenal gland (N), 10 ACA and 10 ACC cases using western blot analysis. β-actin used on the same western blot was used for normalization, whereby the lower band corresponding to the expected ~42 kDa for β-actin was used for quantification and the upper band was the leftover signal from the Complex III band of the total OXPHOS antibody cocktail. (B) Graphs representing quantification of each mitochondrial complexes in each sample group and the difference was evaluated using the Mann-Whitney U-test. (C) Western blot analysis of NDUFC1 in 13 adrenal gland, 25 ACA and 29 ACC samples (from 25 patients with ACC). β-actin used on the same western blot was used for normalization. The three blots shown in the lower panel were from the same blots used in panel A and their β-actin blots are the same as those in panel A. (D) Quantification of NDUFC1 in each group from the blots shown in panel C. P-values were obtained using the Mann-Whitney U-test. (E) Reverse transcription-quantitative PCR of *miR-483-5p* expression in the NCI-H295R ACC cells treated with anti-miR-CTR or anti-miR-483-5p. Error bars represent the SEM of the mean from three independent experiments. P-values were obtained using the Student's t-test. (F) Upper panel, representative western blot image illustrating the effects of anti-miR-483-5p and anti-miR-CTR on NDUFC1 expression. β-actin was used as a loading control. Lower panel, quantification of NDUFC1 levels in *miR-483-5p* inhibition. Error bars represent the SEM of the mean from nine independent experiments. P-values were calculated using the Student's t-test. NDUFC1, NADH:ubiquinone oxidoreductase subunit C1; ACC, adrenocortical carcinoma; ACA, adrenocortical adenoma.

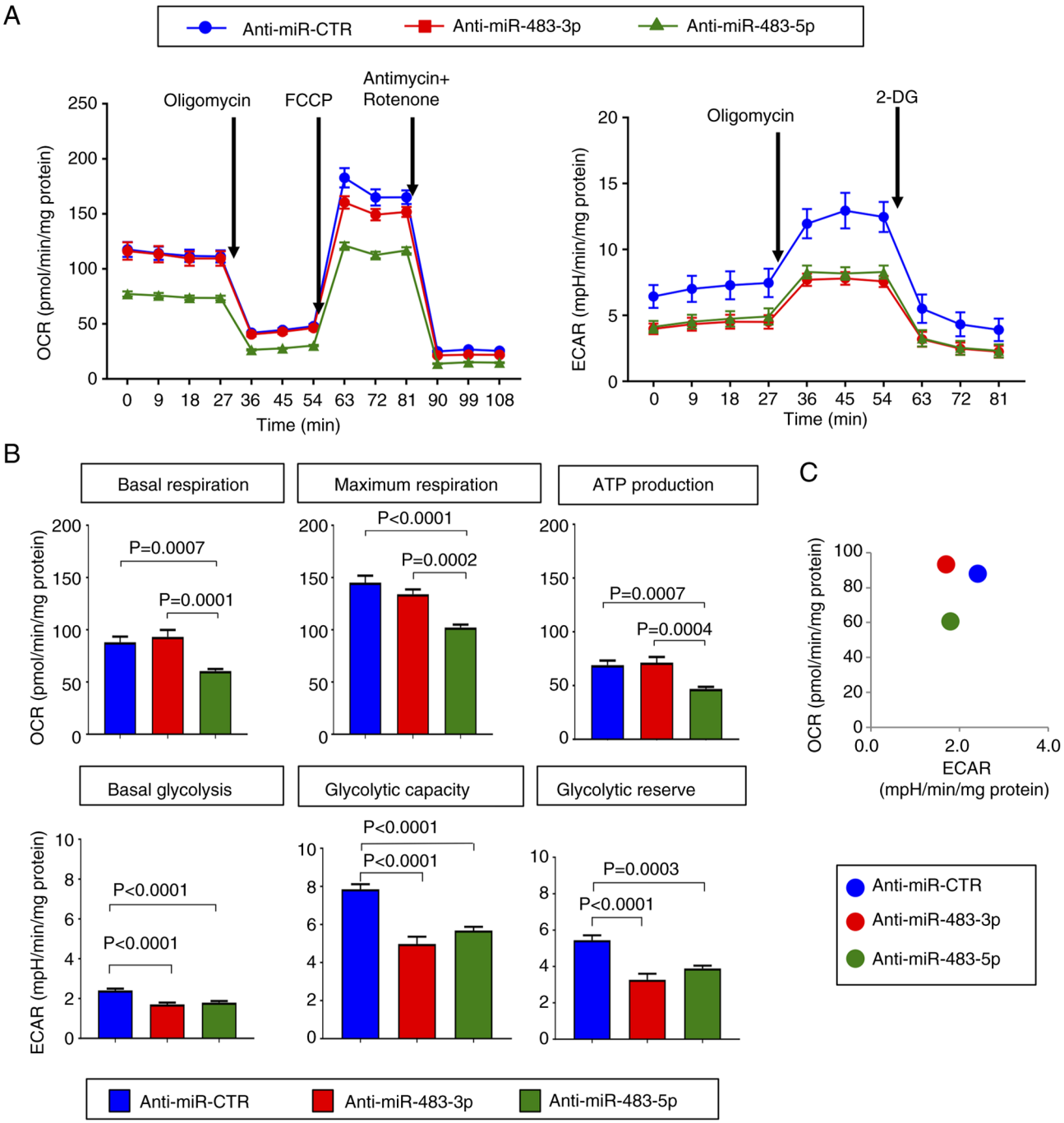

Figure 5. Bioenergetic analysis of *miR-483-3p* or *miR-483-5p* inhibition in the NCI-H295R adrenocortical carcinoma cell line using Seahorse technology. (A and B) OCR and extracellular acidification rate (EACR) were determined in the transfected cells following 72 h of transfection using the Mito Stress test or Glycolysis Stress test, respectively. Values were normalized to total protein content in each well, which were collected after each assay. Error bars represent the SD (n=2). P-values were determined using one-way ANOVA with Tukey's post hoc test. (C) Graph representing the mean OCR and ECAR of the transfected cells at basal conditions. OCR, oxygen consumption rate; EACR, extracellular acidification rate.

It was also demonstrated that *H19* expression was generally higher in ACA compared to normal adrenal, and lower in ACC compared to ACA and normal adrenals. This observation corroborates previous findings of low *H19* levels in some hormonally active ACC (24). Furthermore, the expression of *miR-675* (hosted by *H19*) correlated with *H19* levels in the present cohort and in TCGA dataset.

In the ACC group, the concerted upregulation of *IGF2* together with *miR-483-3p* and *miR-483-5p*, as well as the downregulation of *H19* together with *miR-675* was observed. Each of these molecules could potentially contribute to ACC development alone or cooperatively. The present study then investigated protein expression profiles [obtained using mass spectrometry (41)] of proteins from ACC and ACA, in order to identify proteins that correlate with the transcription from the *H19-IGF2* locus. The correlation analysis of *IGF2* and *H19* transcripts with the proteome took into account both up- and downregulated proteins. Mass spectrometry revealed a correlation between *IGF2* mRNA and IGFII protein levels, as well as an increased IGFII protein content in ACC (Table SIII),

demonstrating that translation of increased *IGF2* mRNAs indeed occur in ACC. Among the 222 proteins overlapping with *IGF2* mRNA expression, 15 proteins (NDUFV1, ANTXR1, RAB20, PTGR1, ECE1, TNS1, MGST1, UGGT1, H6PD, AOC3, TM9SF2, MGST2, SCAMP2, AUP1 and DNAJC16) were significantly downregulated in ACC compared to ACA (Table SIII). One of these, NDUFV1, is associated with mitochondrial oxidative phosphorylation. This indicates that energy metabolism is an important marker for the ACC phenotype.

The present study also applied IPA to the *IGF2* mRNA correlated proteins, to elucidate their associations and ontology. The top two molecular and cellular functions were energy metabolism and lipid metabolism. Further IPA identified hepatocyte nuclear factor 4A and TP53 as the top two upstream regulators, both of which are central to cancer (Table SVII). In addition, IPA suggested seven of the molecules (COX17, NDUFV1, OGDH, PRDX3, TXN2, TXNRD2 and UQCRB) to be associated with mitochondrial dysfunction (Table SVII). Notably, one of the Weiss criteria for the classification of ACC is the presence of <25% clear cells (46). Such tumors instead have a majority of oxyphilic cells, which are characterized by increased amounts of mitochondria (giving the positive eosin staining). It is not known whether these mitochondria are functional or whether they represent a compensatory increase due to a defective mitochondrial function. The present study also found 71 proteins that correlated with *H19* expression, and almost all exhibited a lower prevalence in ACC vs. ACA (Table SIV). Of the 71 identified proteins, 23 displayed significant differences between ACC and ACA. Of note, the protein with the greatest difference between ACC and ACA in association with *H19* transcription is encoded by the potassium channel gene *KCNQ1*, which is imprinted and associated with for example Beckwith-Wiedemann syndrome (47). Other notable proteins are two mitochondrial NDUF (NADH dehydrogenase sub-complex) proteins, supporting the importance of energy metabolism.

As it is assumed that the role of miRNAs is the negative regulation of target genes, the present study analyzed the inverse correlation of these with the proteome. In total, 11 proteins correlated inversely with *miR-675*, one of which was predicted as a target. This apoptosis-related protein, tumor necrosis factor alpha-induced protein 2 (TNFAIP2), is induced by tumor necrosis factor-α and associated with various cancer types (48-50). *miR-483-5p* exhibited an inverse correlation with 101 proteins. By contrast, its companion *miR-483-3p* only negatively correlated with seven proteins. Of note, all except two of these were found in the list of proteins inversely correlating with *miR-483-5p*. However, these two proteins (H6PD and UBE2G2) were not predicted as targets using TargetScan 7.1. The PUMA, a potential target of *miR-483-3p* in ACC (27), was not detected using mass spectrometry. Among the proteins inversely correlating with *miR-483-5p*, a group of mitochondrial proteins/enzymes may be noted, such as members of the NADH dehydrogenase complex, as well as other mitochondrial molecules. In total, 46 of the proteins with an inverse correlation with *miR-483-5p* were differentially expressed between ACC and ACA. This signature was also validated as a classifier for ACC in independent cohorts using TCGA and GTEx datasets. GO analysis revealed the enrichment of biological processes related to mitochondrial respiration. In particular, six subunits of mitochondrial respiratory complex I were downregulated in ACC. The decreased expression of mitochondrial complex I was also validated in an extended series of clinical samples using western blot analysis, suggesting the deficiency of complex I in ACC. In line with these findings, Kimmel *et al* (51) previously demonstrated a poor oxygen uptake by the tumor mitochondria of the rat ACC 494 model using the tricarboxylic acid cycle substrates (α-ketoglutarate, malate and isocitrate), which led them to propose that the tumor mitochondria could be deficiency in the flavoprotein dehydrogeneases for NADH and NADPH oxidation. Notably, the effect of several anti-ACC drugs (mitotane, niclosamide and ATR-101) is also tightly linked to the disruption of mitochondrial function (52-54). In addition, a deficiency in mitochondrial respiratory complex I has also been demonstrated to promote tumor progression in other tumor types, such as breast cancer and hepatoma (55,56).

One of the mitochondrial respiratory complex I subunits, NDUFC1, is also a predicted target of *miR-483-5p*. The expression of this target was upregulated upon *miR-483-5p* inhibition. The involvement of *miR-483-5p* in mitochondrial respiration was also supported by the Mito Stress Test using the Seahorse technology. Additionally, the inhibition of *miR-483-5p* also reduced glycolysis, which led to a low metabolic state resembling cellular quiescence. These results are in line with the observations that the inhibition of *miR-483-5p* had no effect on cell proliferation or apoptosis in ACC (27,30). Although the target(s) of *miR-483-5p* involved in glycolysis remains unknown, the present study noted a common protein, hexose-6-phosphate-dehydrogenase (H6PD), which inversely correlated with both *miR-483-3p* and *miR-483-5p*. H6PD is an enzyme that produces NAPDH in the endoplasmic reticulum for glucose metabolism and glycolysis (57,58). Even though this gene was not predicted as a target of *miR-483-3p* and *miR-483-5p* by TargetScan 7.1, the possibility of H6PD as a direct or indirect target of these miRNAs has not yet been excluded.

The present data may be utilized to identify differentially expressed molecules that may be developed into diagnostic markers for the identification of ACC cases in the absence of metastasis at the time of diagnosis. Furthermore, it may potentially aid in the identification of those patients who could benefit from adjuvant mitotane therapy (59,60). The main findings of the present study were that correlations exist between specific miRNA(s) and RNA(s) in the *IGF2-H19* locus and the proteomes of ACC and ACA. The patterns of RNA transcription from this locus form specific networks of protein expression that appear to be associated with ACC. The present study also reveals a link of the *IGF2-H19* locus to energy metabolism and deficiency of mitochondrial respiratory complex I in ACC, suggesting the importance of mitochondrial dysfunction and *IGF2-H19* regulatory network in ACC development.

Acknowledgements

The authors would like to thank Ms. Lisa Ånfalk (Karolinska University Hospital) for assisting with the collection of all tissue samples, and the Strategic Research Programme Diabetes Facility for the Seahorse system.

Funding

The present study was supported by grants from the Swedish Research Council (2021-03006), the Swedish Cancer Society (20 0843 and 20 0859), the Cancer Society in Stockholm (201223), the Gustav V Jubilee Foundation (204103), the Stockholm County Council (RS 2019-1054) and Funds from Karolinska Institutet (2020-01851 and 2020-01768).

Availability of data and materials

The analyzed datasets presented in the present study are available in the Gene Expression Profiling Interactive Analysis (http://gepia.cancer-pku.cn/), StarBase Pan-Cancer Analysis Platform (https://starbase.sysu.edu.cn/panCancer.php) and ProteomeXchange Consortium (http://proteomecentral.proteomexchange.org; PXD000604).

Authors' contributions

PS, TJE, RB, WOL and CL conceived and designed the study. PS, SC, HK, CX, RF, MoA, JG, HS and MaA performed the experiments and analyzed the data. MK, AH, JZ and RB contributed to the clinical materials and data. WOL and CL supervised the study, and reviewed and approved the authenticity of all the raw data. All authors critically reviewed, and have read and approved the final version of the manuscript.

Ethics approval and consent to participate

The use of the tumor samples (Dnr 01-136; Dnr 2020-04226) and normal adrenals (Dnr 01-353; Dnr 2020-04226) in the present study were approved by the Ethics Committee of Karolinska Institutet (Dnr 01-136; Dnr 01-353) and by the Swedish Ethical Review Authority (Dnr 2020-04226). Tissue samples were collected with informed consent and was obtained from the patients prior to surgery.

Patient consent for publication

Not applicable.

Competing interests

The authors declare that they have no competing interests.

References

1. Assié G, Letouzé E, Fassnacht M, Jouinot A, Luscap W, Barreau O, Omeiri H, Rodriguez S, Perlemoine K, René-Corail F, *et al*: Integrated genomic characterization of adrenocortical carcinoma. Nat Genet 46: 607-612, 2014.
2. Juhlin CC, Goh G, Healy JM, Fonseca AL, Scholl UI, Stenman A, Kunstman JW, Brown TC, Overton JD, Mane SM, *et al*: Whole-exome sequencing characterizes the landscape of somatic mutations and copy number alterations in adrenocortical carcinoma. J Clin Endocrinol Metab 100: E493-E502, 2015.
3. Zheng S, Cherniack AD, Dewal N, Moffitt RA, Danilova L, Murray BA, Lerario AM, Else T, Knijnenburg TA, Ciriello G, *et al*: Comprehensive pan-genomic characterization of adrenocortical carcinoma. Cancer Cell 29: 723-736, 2016.
4. Boulle N, Logié A, Gicquel C, Perin L and Le Bouc Y: Increased levels of insulin-like growth factor II (IGF-II) and IGF-binding protein-2 are associated with malignancy in sporadic adrenocortical tumors. J Clin Endocrinol Metab 83: 1713-1720, 1998.
5. Gicquel C, Bertagna X, Schneid H, Francillard-Leblond M, Luton JP, Girard F and Le Bouc Y: Rearrangements at the 11p15 locus and overexpression of insulin-like growth factor-II gene in sporadic adrenocortical tumors. J Clin Endocrinol Metab 78: 1444-1453, 1994.
6. Gicquel C, Raffin-Sanson ML, Gaston V, Bertagna X, Plouin PF, Schlumberger M, Louvel A, Luton JP and Le Bouc Y: Structural and functional abnormalities at 11p15 are associated with the malignant phenotype in sporadic adrenocortical tumors: Study on a series of 82 tumors. J Clin Endocrinol Metab 82: 2559-2565, 1997.
7. Larsson C: Epigenetic aspects on therapy development for gastroenteropancreatic neuroendocrine tumors. Neuroendocrinology 97: 19-25, 2013.
8. Brannan CI, Dees EC, Ingram RS and Tilghman SM: The product of the H19 gene may function as an RNA. Mol Cell Biol 10: 28-36, 1990.
9. Ogawa O, Eccles MR, Szeto J, McNoe LA, Yun K, Maw MA, Smith PJ and Reeve AE: Relaxation of insulin-like growth factor II gene imprinting implicated in Wilms' tumour. Nature 362: 749-751, 1993.
10. Rainier S, Johnson LA, Dobry CJ, Ping AJ, Grundy PE and Feinberg AP: Relaxation of imprinted genes in human cancer. Nature 362: 747-749, 1993.
11. Weksberg R, Shen DR, Fei YL, Song QL and Squire J: Disruption of insulin-like growth factor 2 imprinting in Beckwith-Wiedemann syndrome. Nat Genet 5: 143-150, 1993.
12. Pravtcheva DD and Wise TL: Metastasizing mammary carcinomas in H19 enhancers-Igf2 transgenic mice. J Exp Zool 281: 43-57, 1998.
13. Veronese A, Lupini L, Consiglio J, Visone R, Ferracin M, Fornari F, Zanesi N, Alder H, D'Elia G, Gramantieri L, *et al*: Oncogenic role of miR-483-3p at the IGF2/483 locus. Cancer Res 70: 3140-3149, 2010.
14. Drelon C, Berthon A, Ragazzon B, Tissier F, Bandiera R, Sahut-Barnola I, de Joussineau C, Batisse-Lignier M, Lefrancois-Martinez AM, Bertherat J, *et al*: Analysis of the role of Igf2 in adrenal tumour development in transgenic mouse models. PLoS One 7: e44171, 2012.
15. Heaton JH, Wood MA, Kim AC, Lima LO, Barlaskar FM, Almeida MQ, Fragoso MC, Kuick R, Lerario AM, Simon DP, *et al*: Progression to adrenocortical tumorigenesis in mice and humans through insulin-like growth factor 2 and β-catenin. Am J Pathol 181: 1017-1033, 2012.
16. Barlaskar FM, Spalding AC, Heaton JH, Kuick R, Kim AC, Thomas DG, Giordano TJ, Ben-Josef E and Hammer GD: Preclinical targeting of the type I insulin-like growth factor receptor in adrenocortical carcinoma. J Clin Endocrinol Metab 94: 204-212, 2009.
17. Fassnacht M, Berruti A, Baudin E, Demeure MJ, Gilbert J, Haak H, Kroiss M, Quinn DI, Hesseltine E, Ronchi CL, *et al*: Linsitinib (OSI-906) versus placebo for patients with locally advanced or metastatic adrenocortical carcinoma: A double-blind, randomised, phase 3 study. Lancet Oncol 16: 426-435, 2015.
18. Haluska P, Worden F, Olmos D, Yin D, Schteingart D, Batzel GN, Paccagnella ML, de Bono JS, Gualberto A and Hammer GD: Safety, tolerability, and pharmacokinetics of the anti-IGF-1R monoclonal antibody figitumumab in patients with refractory adrenocortical carcinoma. Cancer Chemother Pharmacol 65: 765-773, 2010.
19. Jones RL, Kim ES, Nava-Parada P, Alam S, Johnson FM, Stephens AW, Simantov R, Poondru S, Gedrich R, Lippman SM, *et al*: Phase I study of intermittent oral dosing of the insulin-like growth factor-1 and insulin receptors inhibitor OSI-906 in patients with advanced solid tumors. Clin Cancer Res 21: 693-700, 2015.
20. Lerario AM, Worden FP, Ramm CA, Hesseltine EA, Stadler WM, Else T, Shah MH, Agamah E, Rao K and Hammer GD: The combination of insulin-like growth factor receptor 1 (IGF1R) antibody cixutumumab and mitotane as a first-line therapy for patients with recurrent/metastatic adrenocortical carcinoma: A multi-institutional NCI-sponsored trial. Horm Cancer 5: 232-239, 2014.
21. Naing A, Kurzrock R, Burger A, Gupta S, Lei X, Busaidy N, Hong D, Chen HX, Doyle LA, Heilbrun LK, *et al*: Phase I trial of cixutumumab combined with temsirolimus in patients with advanced cancer. Clin Cancer Res 17: 6052-6060, 2011.
22. Ilvesmäki V, Kahri AI, Miettinen PJ and Voutilainen R: Insulin-like growth factors (IGFs) and their receptors in adrenal tumors: High IGF-II expression in functional adrenocortical carcinomas. J Clin Endocrinol Metab 77: 852-858, 1993.

23. Laurell C, Velázquez-Fernández D, Lindsten K, Juhlin C, Enberg U, Geli J, Höög A, Kjellman M, Lundeberg J, Hamberger B, *et al*: Transcriptional profiling enables molecular classification of adrenocortical tumours. Eur J Endocrinol 161: 141-152, 2009.
24. Liu J, Kahri AI, Heikkilä P, Ilvesmäki V and Voutilainen R: H19 and insulin-like growth factor-II gene expression in adrenal tumors and cultured adrenal cells. J Clin Endocrinol Metab 80: 492-496, 1995.
25. Bartel DP: MicroRNAs: Genomics, biogenesis, mechanism, and function. Cell 116: 281-297, 2004.
26. Doghman M, El Wakil A, Cardinaud B, Thomas E, Wang J, Zhao W, Peralta-Del Valle MH, Figueiredo BC, Zambetti GP and Lalli E: Regulation of insulin-like growth factor-mammalian target of rapamycin signaling by microRNA in childhood adrenocortical tumors. Cancer Res 70: 4666-4675, 2010.
27. Özata DM, Caramuta S, Velázquez-Fernández D, Akçakaya P, Xie H, Höög A, Zedenius J, Bäckdahl M, Larsson C and Lui WO: The role of microRNA deregulation in the pathogenesis of adrenocortical carcinoma. Endocr Relat Cancer 18: 643-655, 2011.
28. Soon PS, Tacon LJ, Gill AJ, Bambach CP, Sywak MS, Campbell PR, Yeh MW, Wong SG, Clifton-Bligh RJ, Robinson BG and Sidhu SB: miR-195 and miR-483-5p identified as predictors of poor prognosis in adrenocortical cancer. Clin Cancer Res 15: 7684-7692, 2009.
29. Patterson EE, Holloway AK, Weng J, Fojo T and Kebebew E: MicroRNA profiling of adrenocortical tumors reveals miR-483 as a marker of malignancy. Cancer 117: 1630-1639, 2011.
30. Agosta C, Laugier J, Guyon L, Denis J, Bertherat J, Libé R, Boisson B, Sturm N, Feige JJ, Chabre O and Cherradi N: MiR-483-5p and miR-139-5p promote aggressiveness by targeting N-myc downstream-regulated gene family members in adrenocortical cancer. Int J Cancer 143: 944-957, 2018.
31. Chabre O, Libé R, Assie G, Barreau O, Bertherat J, Bertagna X, Feige JJ and Cherradi N: Serum miR-483-5p and miR-195 are predictive of recurrence risk in adrenocortical cancer patients. Endocr Relat Cancer 20: 579-594, 2013.
32. Decmann A, Bancos I, Khanna A, Thomas MA, Turai P, Perge P, Pintér JZ, Tóth M, Patócs A and Igaz P: Comparison of plasma and urinary microRNA-483-5p for the diagnosis of adrenocortical malignancy. J Biotechnol 297: 49-53, 2019.
33. Patel D, Boufraqech M, Jain M, Zhang L, He M, Gesuwan K, Gulati N, Nilubol N, Fojo T and Kebebew E: MiR-34a and miR-483-5p are candidate serum biomarkers for adrenocortical tumors. Surgery 154: 1224-1229, 2013.
34. Li H, Yu B, Li J, Su L, Yan M, Zhu Z and Liu B: Overexpression of lncRNA H19 enhances carcinogenesis and metastasis of gastric cancer. Oncotarget 5: 2318-2329, 2014.
35. Tsang WP, Ng EK, Ng SS, Jin H, Yu J, Sung JJ and Kwok TT: Oncofetal H19-derived miR-675 regulates tumor suppressor RB in human colorectal cancer. Carcinogenesis 31: 350-358, 2010.
36. Zhai LL, Wang P, Zhou LY, Yin JY, Tang Q, Zhang TJ, Wang YX, Yang DQ, Lin J and Deng ZQ: Over-expression of miR-675 in formalin-fixed paraffin-embedded (FFPE) tissues of breast cancer patients. Int J Clin Exp Med 8: 11195-11201, 2015.
37. Zhou YW, Zhang H, Duan CJ, Gao Y, Cheng YD, He D, Li R and Zhang CF: miR-675-5p enhances tumorigenesis and metastasis of esophageal squamous cell carcinoma by targeting REPS2. Oncotarget 7: 30730-30747, 2016.
38. He D, Wang J, Zhang C, Shan B, Deng X, Li B, Zhou Y, Chen W, Hong J, Gao Y, *et al*: Down-regulation of miR-675-5p contributes to tumor progression and development by targeting pro-tumorigenic GPR55 in non-small cell lung cancer. Mol Cancer 14: 73, 2015.
39. Schmitz KJ, Helwig J, Bertram S, Sheu SY, Suttorp AC, Seggewiss J, Willscher E, Walz MK, Worm K and Schmid KW: Differential expression of microRNA-675, microRNA-139-3p and microRNA-335 in benign and malignant adrenocortical tumours. J Clin Pathol 64: 529-535, 2011.
40. DeLellis RA, Lloyd RV, Heitz PU and Eng C (eds): Pathology and genetics of tumours of endocrine organs. In World Health Organization Classification of Tumours, 3rd edition. Vol. 8. IARC Press, Lyon, France, 2004.
41. Kjellin H, Johansson H, Höög A, Lehtiö J, Jakobsson PJ and Kjellman M: Differentially expressed proteins in malignant and benign adrenocortical tumors. PLoS One 9: e87951, 2014.
42. Tang Z, Li C, Kang B, Gao G, Li C and Zhang Z: GEPIA: A web server for cancer and normal gene expression profiling and interactive analyses. Nucleic Acids Res 45 (W1): W98-W102, 2017.
43. Li JH, Liu S, Zhou H, Qu LH and Yang JH: starBase v2.0: Decoding miRNA-ceRNA, miRNA-ncRNA and protein-RNA interaction networks from large-scale CLIP-Seq data. Nucleic Acids Res 42 (Database Issue): D92-D97, 2014.
44. Gazdar AF, Oie HK, Shackleton CH, Chen TR, Triche TJ, Myers CE, Chrousos GP, Brennan MF, Stein CA and La Rocca RV: Establishment and characterization of a human adrenocortical carcinoma cell line that expresses multiple pathways of steroid biosynthesis. Cancer Res 50: 5488-5496, 1990.
45. Livak KJ and Schmittgen TD: Analysis of relative gene expression data using real-time quantitative PCR and the 2(-Delta Delta C(T)) method. Methods 25: 402-408, 2001.
46. Weiss LM: Comparative histologic study of 43 metastasizing and nonmetastasizing adrenocortical tumors. Am J Surg Pathol 8: 163-169, 1984.
47. Valente FM, Sparago A, Freschi A, Hill-Harfe K, Maas SM, Frints SGM, Alders M, Pignata L, Franzese M, Angelini C, *et al*: Transcription alterations of KCNQ1 associated with imprinted methylation defects in the Beckwith-Wiedemann locus. Genet Med 21: 1808-1820, 2019.
48. Corrêa GT, Bandeira GA, Cavalcanti BG, de Carvalho Fraga CA, dos Santos EP, Silva TF, Gomez RS, Guimarães AL and De Paula AM: Association of-308 TNF-α promoter polymorphism with clinical aggressiveness in patients with head and neck squamous cell carcinoma. Oral Oncol 47: 888-894, 2011.
49. Schteingart DE, Giordano TJ, Benitez RS, Burdick MD, Starkman MN, Arenberg DA and Strieter RM: Overexpression of CXC chemokines by an adrenocortical carcinoma: A novel clinical syndrome. J Clin Endocrinol Metab 86: 3968-3974, 2001.
50. Shih CM, Lee YL, Chiou HL, Chen W, Chang GC, Chou MC and Lin LY: Association of TNF-alpha polymorphism with susceptibility to and severity of non-small cell lung cancer. Lung Cancer 52: 15-20, 2006.
51. Kimmel GL, Péron FG, Haksar A, Bedigian E, Robidoux WF Jr and Lin MT: Ultrastructure, steroidogenic potential, and energy metabolism of the Snell adrenocortical carcinoma 494. A comparison with normal adrenocortical tissue. J Cell Biol 62: 152-163, 1974.
52. Cheng Y, Kerppola RE and Kerppola TK: ATR-101 disrupts mitochondrial functions in adrenocortical carcinoma cells and in vivo. Endocr Relat Cancer 23: 1-19, 2016.
53. Poli G, Guasti D, Rapizzi E, Fucci R, Canu L, Bandini A, Cini N, Bani D, Mannelli M and Luconi M: Morphofunctional effects of mitotane on mitochondria in human adrenocortical cancer cells. Endocr Relat Cancer 20: 537-550, 2013.
54. Satoh K, Zhang L, Zhang Y, Chelluri R, Boufraqech M, Nilubol N, Patel D, Shen M and Kebebew E: Identification of niclosamide as a novel anticancer agent for adrenocortical carcinoma. Clin Cancer Res 22: 3458-3466, 2016.
55. Lee JH, Lee YK, Lim JJ, Byun HO, Park I, Kim GH, Xu WG, Wang HJ and Yoon G: Mitochondrial respiratory dysfunction induces claudin-1 expression via reactive oxygen species-mediated heat shock factor 1 activation, leading to hepatoma cell invasiveness. J Biol Chem 290: 21421-21431, 2015.
56. Santidrian AF, Matsuno-Yagi A, Ritland M, Seo BB, LeBoeuf SE, Gay LJ, Yagi T and Felding-Habermann B: Mitochondrial complex I activity and NAD+/NADH balance regulate breast cancer progression. J Clin Invest 123: 1068-1081, 2013.
57. Marbet P, Klusonova P, Birk J, Kratschmar DV and Odermatt A: Absence of hexose-6-phosphate dehydrogenase results in reduced overall glucose consumption but does not prevent 11β-hydroxysteroid dehydrogenase-1-dependent glucocorticoid activation. FEBS J 285: 3993-4004, 2018.
58. Marini C, Ravera S, Buschiazzo A, Bianchi G, Orengo AM, Bruno S, Bottoni G, Emionite L, Pastorino F, Monteverde E, *et al*: Discovery of a novel glucose metabolism in cancer: The role of endoplasmic reticulum beyond glycolysis and pentose phosphate shunt. Sci Rep 6: 25092, 2016.
59. Berruti A, Grisanti S, Pulzer A, Claps M, Daffara F, Loli P, Mannelli M, Boscaro M, Arvat E, Tiberio G, *et al*: Long-term outcomes of adjuvant mitotane therapy in patients with radically resected adrenocortical carcinoma. J Clin Endocrinol Metab 102: 1358-1365, 2017.
60. Calabrese A, Basile V, Puglisi S, Perotti P, Pia A, Saba L, Berchialla P, Porpiglia F, Veltri A, Volante M, *et al*: Adjuvant mitotane therapy is beneficial in non-metastatic adrenocortical carcinoma at high risk of recurrence. Eur J Endocrinol 180: 387-396, 2019.

This work is licensed under a Creative Commons Attribution-NonCommercial-NoDerivatives 4.0 International (CC BY-NC-ND 4.0) License.